atmosphere

MDPI

Article

Preparation Methods and Performance Analysis of Polyanthra-Quinone/Carbon Nanotube Composites for Capturing Carbon Dioxide

Zhongcheng Wang *, Jingsong Feng, Xiaoyu Liu and Hao Guo

Merchant Marine College, Shanghai Maritime University, Shanghai 201306, China; 201930110089@stu.shmtu.edu.cn (J.F.); liuxiaoyu@shmtu.edu.cn (X.L.); guohao@shmtu.edu.cn (H.G.)
* Correspondence: wangzhongchengwzc@163.com; Tel.: +86-13816760424

Abstract: Carbon capture is one of the important methods to achieve carbon neutrality. In this paper, a simple and reliable method for the preparation of poly(anthraquinone)/multi-walled carbon nanotube composites (PAQ/MWCNTs) for capturing carbon dioxide is proposed. Using constant magnetic stirring, 1,4-anthraquinone (1,4-AQ) was allowed to accumulate on multi-walled carbon nanotube (MWCNTs) substrates via π–π. The poly(anthraquinone)/multi-walled carbon nanotube composites were produced by this continuous process. Besides, the carbon cloth electrode prepared from PAQ/MWCNTs composites was subjected to redox potentials for carbon dioxide capture. Results showed that PAQ/MWCNTs composites had good redox reversibility, their carbon dioxide capture capacity was 7.80 mmol·g^{-1} while the material utilization rate reaches reached 73.4%.

Keywords: 1,4-anthraquinone; multi-walled carbon nanotubes; magnetic stirring; poly(anthraquinone)/multi-walled carbon nanotube composites; carboxylation; carbon dioxide capture

check for updates

Citation: Wang, Z.; Feng, J.; Liu, X.; Guo, H. Preparation Methods and Performance Analysis of Polyanthra-Quinone/Carbon Nanotube Composites for Capturing Carbon Dioxide. *Atmosphere* **2022**, *13*, 543. https://doi.org/10.3390/atmos13040543

Academic Editors: Hui Xing, Jiaguo Liu and Stephen Spence

Received: 22 February 2022
Accepted: 27 March 2022
Published: 29 March 2022

Publisher's Note: MDPI stays neutral with regard to jurisdictional claims in published maps and institutional affiliations.

Copyright: © 2022 by the authors. Licensee MDPI, Basel, Switzerland. This article is an open access article distributed under the terms and conditions of the Creative Commons Attribution (CC BY) license (https://creativecommons.org/licenses/by/4.0/).

1. Introduction

Climate change is a huge challenge for all mankind, and global warming caused by greenhouse gas emissions endangers the balance of natural ecosystems and even threatens the survival of mankind. President Xi Jinping proposed that China should strive to peak CO_2 emissions by 2030 and achieve carbon neutrality by 2060 [1] at the 75th session of the United Nations General Assembly on 22 September 2020. As of October 2020, 127 countries around the world have made carbon neutral commitments [2] and have formulated development plans to support the development of low/zero carbon technologies. In the peak period of carbon emissions, high-quality peaks need to be balanced with sustainable economic and social development [3]. Carbon capture technologies as an important means of reducing emissions can effectively reduce the pressure on carbon emissions during the peak period.

Many CO_2 capture technologies have been developed over time such as absorption using solid [4] adsorbents or solvents such as amines [5] and lye [6], membrane separation [7], and low-temperature distillation [8]. Adsorption using solid adsorbents is the selective adsorption of CO_2 from a gas mixture, followed by desorption and concentration of CO_2 under specific conditions. Chemical absorption is one of the more widely used and technically mature methods. It uses a chemical solvent to react with CO_2 in a reversible chemical reaction to absorb and desorb CO_2. Membrane technology uses the different particle size and pressure difference requirements for separation and separation requirements to separate and sort materials. The cryogenic separation method is based on the difference in volatility of each gas in the flue gas, and the flue gas is repeatedly compressed and condensed to reach a critical value of CO_2, thus allowing the CO_2 to be converted from a gaseous state to a liquid state and separated from the gas mixture.

Nevertheless, the large energy consumption required for the thermal regeneration of solvents in adsorption and absorption technologies limits their application [9]. Besides, membrane separation technologies are difficult to directly treat flue gases at low CO_2 concentrations [10]. Moreover, low-temperature distillation technologies have complex pretreatment systems, large equipment, high energy consumption, and poor separation results [11]. All the mentioned above CO_2 capture technologies are limited in their application and development due to the large energy consumption associated with heating the solvent and adsorbent, pressurizing the raw gas, or desorption by vacuum.

Due to the problems with existing CO_2 capture technologies, more new technologies are being investigated. The radical dianion, the electrochemical reduction product of quinones, has been shown to be a nucleophilic reagent for capturing carbon dioxide [12]. The carboxylation of reduced quinones can bind to carbon dioxide, which allows quinones to trap carbon dioxide when a reduction potential is applied (as shown in Equation (1)). Correspondingly quinones that bind to carbon dioxide release carbon dioxide when oxidation potential is applied [13].

$$Q + e \rightleftharpoons Q^{-};\ Q^{-} + e \rightleftharpoons Q^{2-};\ Q^{2-} + 2CO_2 \rightleftharpoons [Q - 2CO_2]^{2-} \quad (1)$$

The radical dianion, the electrochemical reduction product of quinones, has been shown to be a nucleophilic reagent for capturing carbon dioxide [12]. The carboxylation of reduced quinones can bind to carbon dioxide, which allows quinones to trap carbon dioxide when a reduction potential is applied (as shown in Equation (1)). Correspondingly quinones that bind to carbon dioxide release carbon dioxide when oxidation potential is applied [13].

The selective capture of carbon dioxide in gas streams by applying high and low potentials to quinone materials has a wider application, whereby the difference in affinity of the quinone redox products for carbon dioxide is taken advantage of when applied at high and low potentials. Besides, this method of capturing carbon dioxide is not easily constrained by the environment and there is no energy loss due to changes in temperature or pressure as compared to other methods. Scovazzo, Poshusta et al. [14] demonstrated that while screening several ionic liquids as suitable electrolytes for quinone carriers in electrochemically mediated CO_2 selective transport systems, it was possible to capture CO_2 in ionic liquids (IL) and organic solvent electrolyte media with 2,6-di-*tert*-butyl-1,4-benzoquinone as a carrier for the electrochemical separation of CO_2 from gas mixtures at concentrations of less than 1%. Grimaud et al. [15] validated the use of quinones as chemical catalysts to promote lithium-CO_2 cells for carbon reduction. The results further confirmed that the radical anion (Q^{-}), the divalent anion (Q^{2-}), and the electroreduction products of quinones, were nice good reagents for carbon dioxide capture. Liu, Ye et al. [16] used a concentrated lithium bis(trifluoromethanesulfonyl)imide (LiTFSI) aqueous electrolyte in the electro-swing reactive adsorption for CO_2 capture to significantly reduce electrolyte costs.

Carbon nanotubes are visualised as a structure of graphite layers folded into carbon cylinders and divided into single-walled carbon tubes (SWNT) and multi-walled carbon tubes (MWNT) [17]. Since their discovery in 1991 [18], carbon nanotubes have rapidly become a hot research topic due to their unique mechanical, electrical, and chemical properties as well as their unique tubular molecular structure and potential applications [19]. Voskian and Hatton [20] studied the electro-swing capture of CO_2. They refer to the study of Yamamoto et al [21]. for metal-organic dehalogenated condensation of dichloroanthraquinone. The produced poly(anthraquinone) was sonicated in N-methyl pyrrolidone (NMP) and then multi-walled carbon nanotubes were sonicated to make polymer-multi-walled carbon nanotube composites(P1,4AQ-CNT).

This paper proposes a method for the preparation of poly(anthraquinone)/carbon nanotube composites that is simpler than the process used by Hatton et al. to prepare polymer-multi-walled carbon nanotube composites. The method can successfully trap CO_2 in lithium bis(trifluoromethanesulfonyl)imide (LiTFSi) aqueous electrolytes by applying high and low potentials to the composites.

2. Materials and Methods

2.1. Reagent

The reagents used in this experiment are shown in Table 1. All solutions for the experiments were prepared from ultrapure water.

Table 1. Reagents and properties.

Reagent Items	Characteristics and Manufacturers, etc.
1,4-anthraquinone	purity > 99.5%, Shanghai Aladdin Biochemical Technology Co., Ltd. (Shanghai, China)
Graphitized multi-walled carbon nanotubes	inner diameter: 5–10 nm, outer diameter: 20–30 nm, length: 10–30 μm, purity > 99.9%, Shanghai Aladdin Biochemical Technology Co., Ltd. (Shanghai, China)
Lithium bis(trifluoromethanesulfonyl)imide	purity > 99.9%, Shanghai Eon Chemical Technology Co., Ltd. (Shanghai, China)
N-methyl-pyrrolidone	purity > 99.5%, Shanghai Maclean Biochemical Technology Co., Ltd. (Shanghai, China)
Carbon dioxide	purity ≥ 99.999%, Shanghai Mizheng Gas Co., Ltd. (Shanghai, China)
Nitrogen	purity ≥ 99.99%, Shanghai Mizheng Gas Co., Ltd. (Shanghai, China)
Carbon paper TGP-H-060	thickness: 0.19 mm, density: 0.44 g/cm, resistivity: 5 mΩ-cm, Toray Corporation (Tokyo, Japan)
Ag/AgCl reference electrode	0.1989 V vs. NHE

2.2. Preparation of Materials

2.2.1. Preparation of PAQ/MWCNTs Composites

100 mg of multi-walled carbon nanotubes and 45 mg of 1,4-AQ were dispersed in a solution containing 50 mL of ethanol-water (1:1). Then, the mixture was sonicated for 20 min to dissolve and disperse well and after that, it was stirred magnetically at room temperature for 24 h. After centrifugal separation, a wet mixture was obtained and dried in a vacuum oven at 80 °C for 10 h to give the final product which is the solid powder. An overview of the process is shown in Figure 1. The product after centrifugal separation is shown in Figure 2a while the product after drying is shown in Figure 2b.

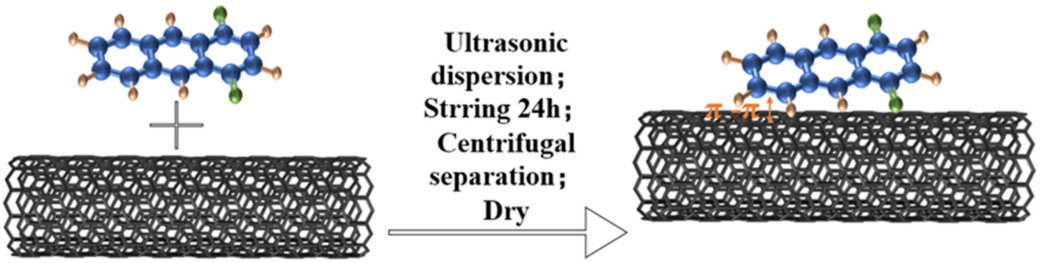

Figure 1. Schematic diagram of the synthesis of PAQ/MWCNTs composites.

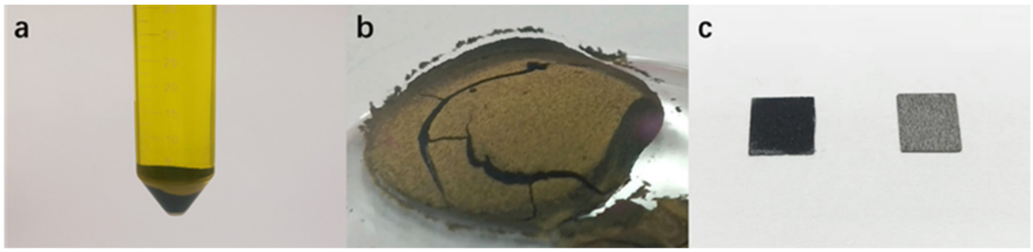

Figure 2. (**a**) The solvent and precipitation after centrifugal separation; (**b**) PAQ/MWCNTs composites; (**c**) PAQ/MWCNTs modified electrode (**left**) and carbon cloth electrode (**right**). This figure was created by the author.

2.2.2. Preparation of PAQ/MWCNTs Modified Electrode

40 mg of the above PAQ/MWCNTs composites solid powder was dissolved in 10 mL NMP and the mixture was sonicated for 10 min to obtain a uniform dispersion. 20 μL of the dispersion was added dropwise on the surface of 1 cm^2 of conductive carbon paper,

dried at 120 °C under normal pressure for 15 min, removed and added dropwise again to the dispersion, dried again, and repeated until the third dropwise was added. After that, the electrode was finally dried at 120 °C for 120 min under normal pressure to produce a working electrode with a loading mass of 0.2 mg·cm^{-1}. The prepared PAQ/MWCNTs modified electrode is shown on the left in Figure 2c and the electrode before preparation is shown on the right in Figure 2c.

2.3. Electrochemical Experiments

2.3.1. Electrochemical Performance Test

In order to examine the reversible nature and redox potential of the PAQ/MWCNTs composites for electrochemical capture of carbon dioxide, the electrochemical performance test of PAQ/MWCNTs composites in the three-electrodes system was designed as shown in Figure 3. Cyclic voltammetry scans were performed using three different electrodes including PAQ/MWCNTs modified electrode as the working electrode, platinum electrode as the auxiliary electrode, and Ag/AgCl as the reference electrode. The three electrodes were placed in a 20 M lithium bis(trifluoromethanesulfonyl)imide electrolyte under the conditions of nitrogen and carbon dioxide inlet.

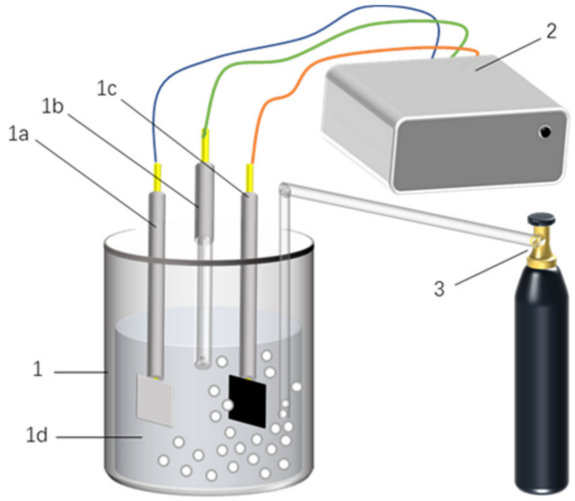

Figure 3. Schematic diagram of three electrodes test system (1—the electrolytic cell; 1a—platinum electrodes; 1b—Ag/AgCl reference electrodes; 1c—PAQ/MWCNTs modified electrode; 1d—lithium bis(trifluoromethanesulfonyl)imide electrolyte; 2—electrochemical workstation; 3—gas cylinders and lines).

2.3.2. Carbon Dioxide Capture and Thermal Regeneration Experiments

Thermal regeneration and electrochemical experiments were designed to test the carbon dioxide capture capacity of the composites (as shown in Figure 4). Carbon dioxide capture was first performed by cyclic voltammetry scanning of the electrode material with a mass of 0.2 mg and an area of 1 cm^2 at a scanning rate of 25 mV·s^{-1} in the range of −0.4 V to 0 V, which can be determined by the reduction potential from the electrochemical performance test. The reduced working electrode was placed in a nitrogen-filled headspace vial, which was then placed in a desiccator and stored at 120 °C at atmospheric pressure, allowing the carbon dioxide to be re-released. The gas in the headspace bottle was sampled and analyzed using a gas chromatograph.

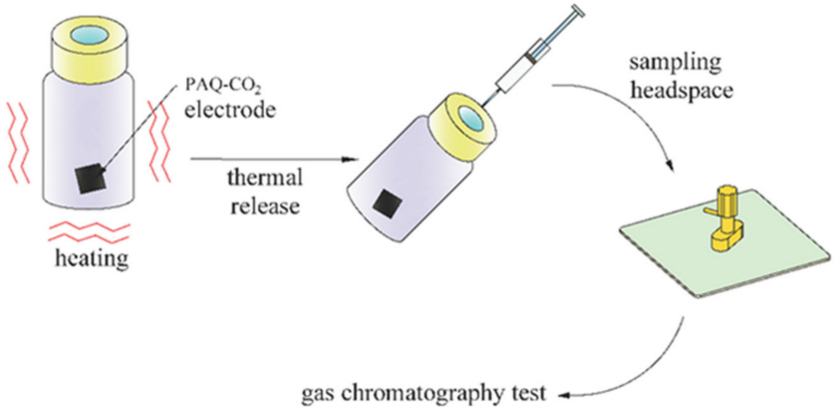

Figure 4. Flow chart of thermal-released CO_2.

The thermally regenerated electrode material was cyclic voltammetry scanned at 25 mV·s^{-1} scan rate in the range of −0.5 V to 0.4 V (determined by the redox potential from electrochemical performance testing). The peak area ratio near the oxidation potential was observed to determine the proportion of captured CO_2 thermally regenerated.

2.4. Test Equipment and Conditions

The IR spectra of 1,4-anthraquinone and poly-1,4-anthraquinone/multi-walled carbon nanotube composites were tested using an IR/Nicolet 6700 FTIR spectrometer (Thermo Fisher Scientific, Waltham, MA, USA) with a resolution setting of 4 cm^{-1}, and a sample scan number of 32. transmission electron microscopy was performed using a JEM-2100F (JEOL, Tokyo, Japan) was used for transmission electron microscopy testing of 1,4 anthraquinone and PAQ/MWCNTs composites, respectively.

Cyclic voltammetry scanning under carbon dioxide and nitrogen conditions was performed using a Zennium electrochemical workstation (Zahner, Kronach, Germany) with a three-electrode system: a PAQ/MWCNTs modified working electrode, an Ag/AgCl reference electrode and a platinum sheet auxiliary electrode, a 20 M lithium bis(trifluoromethanesulfonyl)imide aqueous electrolyte, and a scan rate of 25 mV s^{-1}.

Carbon dioxide concentration was tested using GC-14B gas chromatograph (Shimadzu, Kyoto, Japan), detector: FID; packed column: TDX-02 2 m × 2 mm; inlet temperature: 100 °C; column temperature: 100 °C; detector temperature: 250 °C; carrier gas: 99.999% argon, flow rate: 30 mL/min; methane conversion oven temperature: 380 °C.

The performance parameters of the above instruments are shown in the Supplementary Materials, Tables S1–S4.

3. Results and Discussion

3.1. FTIR Spectra of 1,4-AQ and PAQ/MWCNTs Composites

The FTIR spectra of 1,4-AQ and PAQ/MWCNTs composites are shown in Figure 5. The characteristic peak of the stretching vibration of the C–H bond located on the benzene ring is present at the wavenumber of 3054.88 cm^{-1} while the characteristic peak of the stretching vibration of the C=O group of anthraquinone is present at the wavenumber of 1666.14 cm^{-1}. In addition, and the out-of-plane bending vibration peak of the C–H bond located on the benzene ring is present at the wavenumber of 702.18 cm^{-1}. Among them, the intensity of the C-H characteristic peaks represented by 3054.88 cm^{-1} and 702.18 cm^{-1} is weakened-indicating that 1,4-AQ and multi-walled carbon nanotubes are bonded by π–π bonds, and 1,4-AQ is successfully modified on the MWCNT surface to form PAQ-MWCNT composites [22].

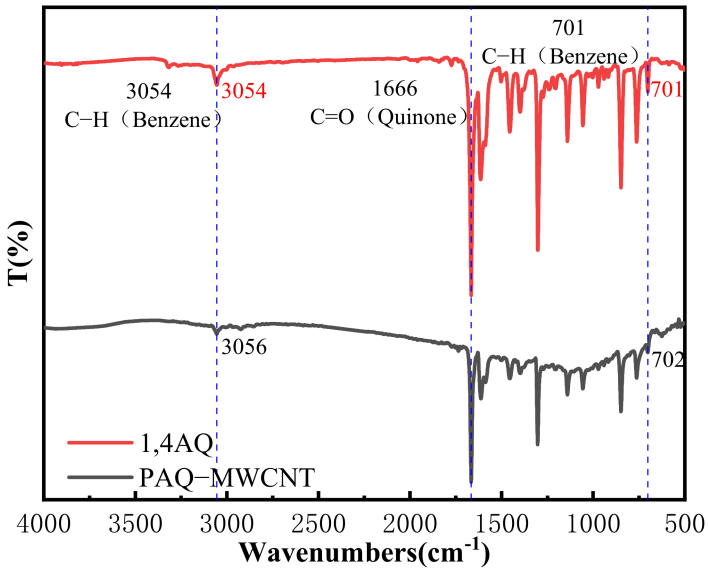

Figure 5. FTIR spectra of 1,4-AQ and PAQ/MWCNTs composites.

3.2. TEM Characterization of PAQ/MWCNTs Composites

To further observe the morphological characteristics of the PAQ/MWCNTs composites, TEM tests were performed on the prepared PAQ/MWCNTs composites and the pre-prepared 1,4-AQ. The TEM images of a single pre-prepared multi-walled carbon nanotube are shown in Figure 6a,c while the TEM images of a single multi-walled carbon nanotube modified with poly(anthraquinone) are illustrated in Figure 6b,d. From Figure 6d, a poly (1,4-anthraquinone) layer with a distinctly different level from the multi-walled carbon nanotube and a width of about 2 nm appears clinging to the multi-walled carbon nanotube wall. Because of the presence of large π-bonds in the meso-phenylene ring functional group of 1,4-AQ and on the graphitized multi-walled carbon nanotubes, the π–π interactions cause the 1,4-AQ to continuously polymerize on the multi-walled carbon nanotube walls when the two materials are mixed and stirred sufficiently for a long time [22]. The infrared spectroscopy tests presented previously in Section 3.1. also yielded similarly consistent conclusions. Such a good structure of anthraquinone-coated carbon nanotubes can combine electrical conductivity with the contact of carbon dioxide with anthraquinone [23].

3.3. CV Testing of PAQ/MWCNTs Composites

In the presence of CO_2, a single two-electron quasi-reversible reduction of quinone in a nonprotonic electrolyte occurs at the first reduction potential, where the CO_2 molecule carboxylates the quinone to produce carbonate [12]. The quinone molecule produces a semi-quinone radical anion on the first reduction. Some semiquinones with sufficient electron density (i.e., sufficient Lewis base strength) can react with CO_2 in a nucleophilic addition to produce carbonates [24]. However, semiquinones with lower electron density do not have the nucleophilic strength to react with CO_2 due to the attached electron attracting groups. After carboxylation of the semiquinone by reductive addition of CO_2, its negative charge is separated from the rest of the molecule by an s-bond, making the carboxylated quinone aromatic ring relatively neutral. Therefore, the two-electron reduction of the parent quinone under CO_2 occurs at the first reduction potential, as shown in Figure 7. Furthermore, the second reduction produces another nucleophilic center, the second oxygen of the quinone, which reacts with the second CO_2 molecule to form the quinone double anion diadduct [25].

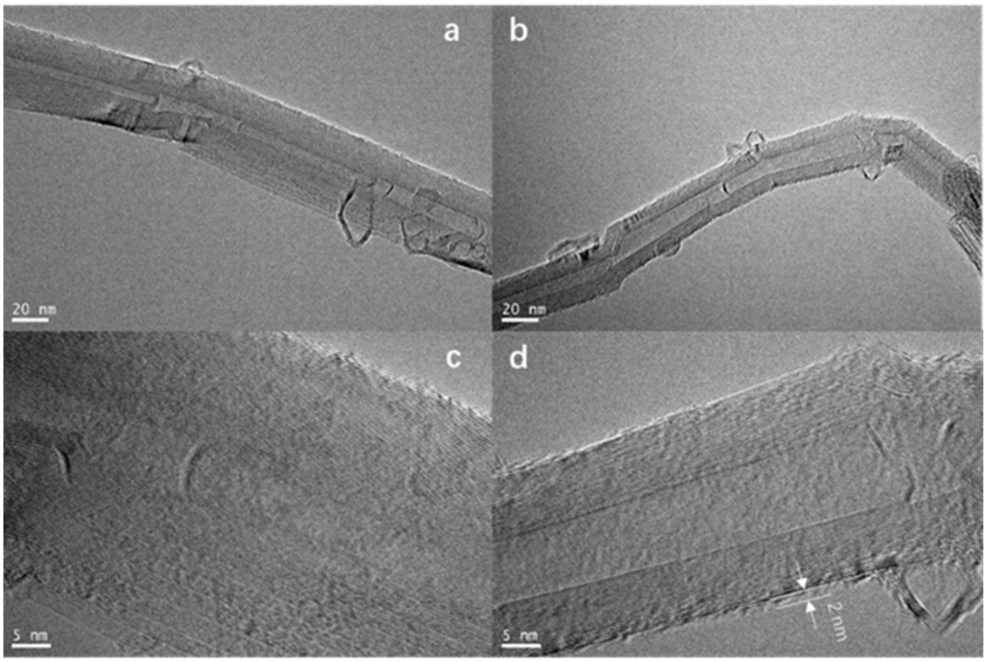

Figure 6. TEM of MWCNTs (**a**,**c**) and TEM of PAQ/MWCNTs composites (**b**,**d**). This figure was created by the author.

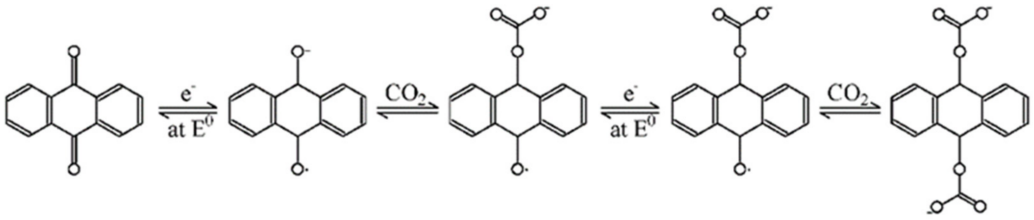

Figure 7. Reduction principle of anthraquinone in the presence of CO_2.

The CV test curves of the PAQ/MWCNTs composites made in this experiment under nitrogen and carbon dioxide environments are shown in Figure 8. The cyclic voltammetry characteristic curves of the composites have significant symmetry. Under CO_2 conditions, the values of the anodic peak current Ipa, the cathodic peak current Ipc, the anodic peak potential Epa, and the reduction potential Epc are 1.392 mA, 1.450 mA, 0.065 V, and −0.190 V, respectively. The good symmetry of the cyclic voltammetry characteristic curves verifies that the quinone electrochemical capture of the CO_2 process is reversible. The anodic peak potential of the composite under CO_2 conditions is significantly positively shifted compared to that under nitrogen conditions (from −0.251 V to 0.065 V). This indicates that the reduced quinone undergoes carboxylation at the oxidation potential under CO_2 conditions, i.e., a PAQ-CO_2 adduct is formed with CO_2, and this process requires an additional driving force for oxidation compared to the formation of the quinone dianion [16].

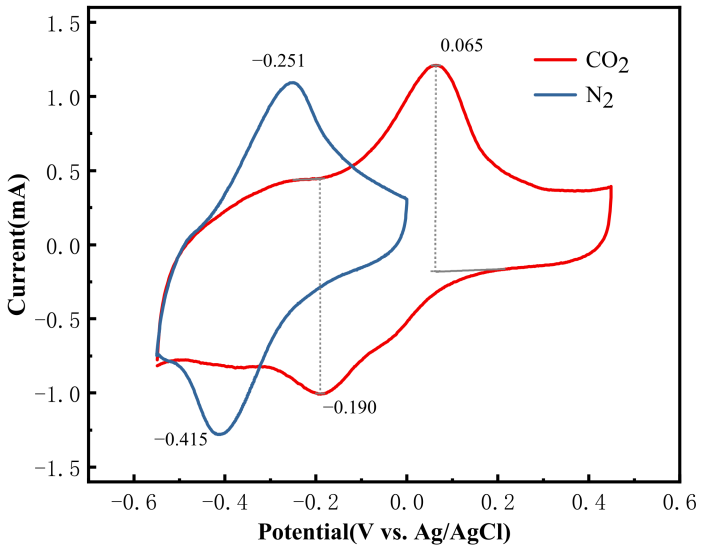

Figure 8. Cyclic voltammograms of PAQ/MWCNTs composite electrodes in nitrogen and carbon dioxide.

3.4. Electrochemical CO_2 Capture Effect Test

3.4.1. CV Tests before and after Thermal Regeneration of the Material Electrode

The redox potential of the PAQ/MWCNTs composite electrodes was obtained through the previous cyclic voltammetry tests, which was performed at its reduction potential and allowed the electrode to capture carbon dioxide. From Figure 9, no significant reduction peak is observed anymore after doing the cyclic voltammetry scans five consecutive times in the range of −0.4 V to 0 V. This proves that the electrode material has trapped CO_2 close to saturation, i.e., the complete formation of the PAQ-CO_2 adduct.

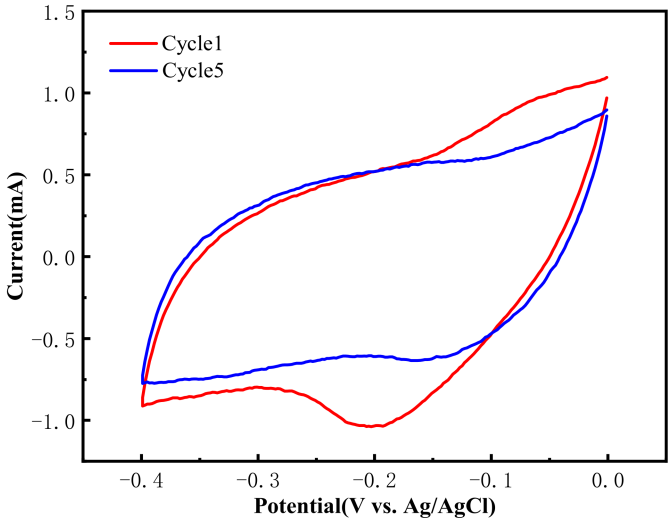

Figure 9. Cyclic voltammograms of PAQ/MWCNTs composite electrodes at reduction potential.

The above PAQ-CO_2 electrode material was thermally regenerated at 120 °C before conducting the cyclic voltammetry scanning in the range of −0.5 V to 0.4 V. As shown in Figure 10, a higher oxidation current appears near the oxidation potential at the beginning of the first cycle compared to the later cycling process-indicating that the electrochemically captured CO_2 is not completely released during the thermal regeneration, around 10% of the captured CO_2 remains in the PAQ-CO_2 electrode material.

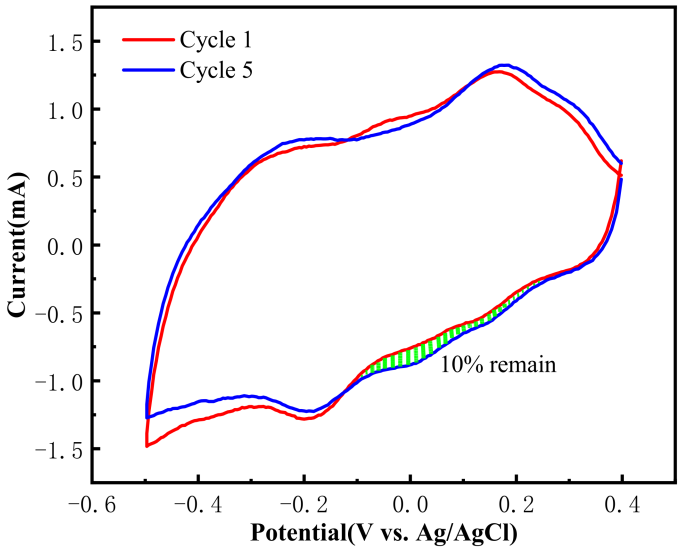

Figure 10. Cyclic voltammograms of PAQ/MWCNTs composite electrodes after 120 °C thermal release.

3.4.2. CO_2 Capture Capacity

It is well known that the molecular weight n of 1,4-AQ is 216 g/mol and the molar volume of the standard gas V_m is 22.4 L. Assuming that the mass of PAQ in the PAQ/MWCNTs composite is m, the theoretical volume of carbon dioxide absorbed by a working electrode loaded with 0.2 mg of PAQ/MWCNTs composite (mass ratio: PAQ:MWCNTs = 1:1) should be:

$$V = \frac{2m}{n} V_m = \frac{0.1 \times 10^{-3} \times 2}{216} \times 22.4 \times 10^6 = 20.7\ \mu L \quad (2)$$

Likewise, the theoretical CO_2 uptake capacity of PAQ/MWCNTs can be obtained as 9.26 mmol·g^{-1}. As shown in Figure 11 and Table 2, the ratio of the peak areas of the chromatograms of the sample and the standard gas yields a CO_2 content of 13.7 μL in the sample. Moreover, since 10% CO_2 remained in the electrode material after the thermal regeneration electrochemical test, the actual CO_2 capture capacity of the prepared PAQ/MWCNTs composite is converted to 7.80 mmol·g^{-1} (per gram of anthraquinone as a reference, hereinafter), which has a theoretical value of about 73.4%.

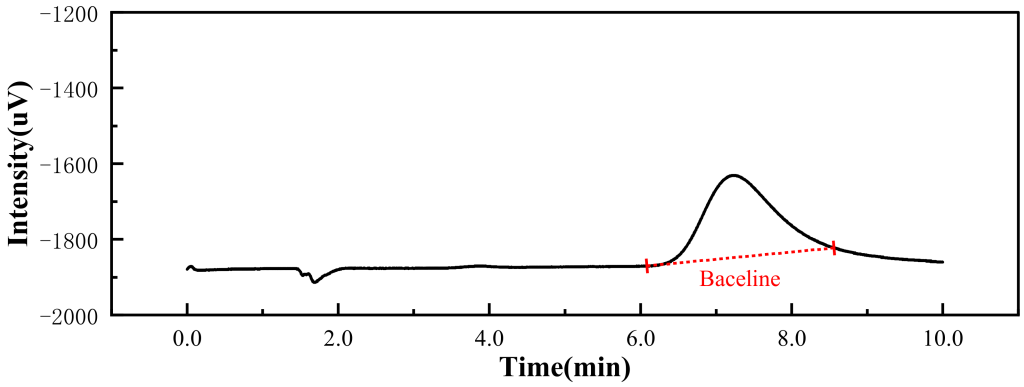

Figure 11. Chromatogram of thermal released carbon dioxide/nitrogen samples.

Table 2. Results of gas chromatographic analysis.

Individual Parts	Retention Time (min)	Peak Height (uV)	Peak Area (uV·s)	Actual Concentration (%)
Carbon dioxide	7.228	217	13,754	0.137

The actual capacity of the material is 7.80 mmol·g^{-1}, which is slightly below the maximum CO_2 capture capacity of existing industrial use of hydramine, which is 8 mmol·g^{-1} [26]. Although the actual capture capacity of the material proposed in this paper is slightly lower than the highest industrial capacity currently, the ideal capture capacity of the material, i.e., 9.26 mmol·g^{-1}, is in excess of the highest industrial capture capacity. It is assumed that with adjustments to the preparation conditions, such as the proportion of raw materials and the mixing time, the actual capture capacity is expected to be closer to the ideal value, thus exceeding the existing industrial CO_2 capture capacity.

4. Conclusions

In this paper, poly(anthraquinone)/multi-walled carbon nanotube composites were successfully prepared by π–π stacking using magnetic stirring method. Besides, their structures were analyzed by means of Fourier infrared spectroscopy and transmission electron microscopy tests. Moreover, PAQ/MWCNTs were loaded onto the surface of carbon cloth electrode at 0.02 mg·cm^2, and carbon dioxide capture under electrochemical conditions was performed using the electrode of this material. The main conclusions are as follows:

1. The material is structurally composed of poly(anthraquinone) with a width of about 2 nm covered by multi-walled carbon nanotubes. Besides, electrochemically, the material had good redox reversibility, its carbon dioxide capture capacity was 7.80 mmol·g^{-1} with 73.4% material utilization;
2. The magnetic stirring method proposed in this experiment was simpler in terms of steps as compared with the metal-organic dehalogenated polycondensation and the combined ultrasonication method used by previous researchers.

Supplementary Materials: The following supporting information can be downloaded at: https://www.mdpi.com/article/10.3390/atmos13040543/s1, Table S1. Technical indicators of the IR/Nicolet 6700 Fourier transform infrared spectrometer; Table S2. Technical indicators of JEM-2100F transmission electron microscopy; Table S3. Technical indicators of Zennium electrochemical workstation; Table S4. Technical indicators of GC-14B gas chromatograph.

Author Contributions: Conceptualization, Z.W. and J.F.; methodology, J.F.; validation, J.F., H.G. and Z.W.; formal analysis, H.G.; data curation, J.F.; writing—original draft preparation, J.F.; writing—review and editing, Z.W.; supervision, Z.W. and X.L.; project administration, Z.W. All authors have read and agreed to the published version of the manuscript.

Funding: This research was funded by the Science & Technology Commission of Shanghai Municipality and Shanghai Engineering Research Center of Ship Intelligent Maintenance and Energy Efficiency, grant number 20DZ2252300.

Institutional Review Board Statement: Not applicable.

Informed Consent Statement: Not applicable.

Data Availability Statement: Not applicable.

Acknowledgments: Financial support from the Science & Technology Commission of Shanghai Municipality is gratefully acknowledged. Special thanks to College of Ocean Science and Engineering and the Laboratory Management Office of Shanghai Maritime University for their support with reagents and instrumentation.

Conflicts of Interest: The authors declare no conflict of interest.

References

1. People's Network. Database of Xi Jinping's Series of Important Speeches. Available online: http://jhsjk.people.cn/ (accessed on 5 September 2021).
2. Wang, C.; Zhang, Y. The path to carbon neutral vision and policy system. *China Environ. Manag.* **2020**, *12*, 58–64. [CrossRef] [PubMed]
3. Xian, X.; Guo, S.; Kong, H.; Zhao, W.; Li, J.; Liu, J.; Zhong, P. Science and technology needs and technology pathways for carbon neutral vision. *China Environ. Manag.* **2021**, *13*, 65–70. [CrossRef]

4. Seah, G.L.; Wang, L.; Tan, L.F.; Tipjanrawee, C.; Sasangka, W.A.; Usadi, A.K.; McConnachie, J.M.; Tan, K.W. Ordered Mesoporous Alumina with Tunable Morphologies and Pore Sizes for CO_2 Capture and Dye Separation. *ACS Appl. Mater. Interfaces* **2021**, *13*, 36117–36129. [CrossRef]
5. Luis, P. Use of monoethanolamine (MEA) for CO_2 capture in a global scenario: Consequences and alternatives. *Desalination* **2016**, *380*, 93–99. [CrossRef]
6. Wang, Z.; Liu, X.; Zhou, P.; Xu, L. Impacts of CaO solid particles in carbon dioxide absorption process from ship emission with NaOH solution. *J. Shanghai Jiaotong Univ.* **2018**, *23*, 320–326. [CrossRef]
7. Wang, H.; He, S.; Qin, X.; Li, C.; Li, T. Interfacial engineering in metal–organic framework-based mixed matrix membranes using covalently grafted polyimide brushes. *J. Am. Chem. Soc.* **2018**, *140*, 17203–17210. [CrossRef]
8. Yousef, A.M.; El-Maghlany, W.M.; Eldrainy, Y.A.; Attia, A. New approach for biogas purification using cryogenic separation and distillation process for CO_2 capture. *Energy* **2018**, *156*, 328–351. [CrossRef]
9. Baena-Moreno, F.M.; Rodríguez-Galán, M.; Vega, F.; Alonso-Fariñas, B.; Arenas, L.F.V.; Navarrete, B. Carbon capture and utilization technologies: A literature review and recent advances. *Energy Sources Part A Recovery Util. Environ. Eff.* **2019**, *41*, 1403–1433. [CrossRef]
10. Xu, S.; Han, C.; Zhang, L.; Zhang, Y.; Du, D.; He, S.; Luo, Y. Advances in carbon dioxide separation and capture. *Nat. Gas Chem. Ind.* **2011**, *36*, 72–78. [CrossRef]
11. Bai, L.; Zhang, X.; Deng, J. Ionic liquids based membranes for CO_2 separation: A review. *CIESC J.* **2016**, *7*, 248–257. [CrossRef]
12. Mizen, M.B.; Wrighton, M.S. Reductive Addition of CO_2 to 9, 10-Phenanthrenequinone. *J. Electrochem. Soc.* **1989**, *136*, 941. [CrossRef]
13. Rheinhardt, J.H.; Singh, P.; Tarakeshwar, P.; Buttry, D.A. Electrochemical capture and release of carbon dioxide. *ACS Energy Lett.* **2017**, *2*, 454–461. [CrossRef]
14. Scovazzo, P.; Poshusta, J.; DuBois, D.; Koval, C.; Noble, R. Electrochemical separation and concentration of<1% carbon dioxide from nitrogen, J. *Electrochem. Soc.* **2013**, *150*, D91. [CrossRef]
15. Yin, W.; Grimaud, A.; Azcarate, I.; Yang, C.; Tarascon, J.M. Electrochemical reduction of CO_2 mediated by quinone derivatives: Implication for Li–CO_2 battery. *J. Phys. Chem. C* **2018**, *122*, 6546–6554. [CrossRef]
16. Liu, Y.; Ye, H.Z.; Diederichsen, K.M.; van Voorhis, T.; Hatton, T.A. Electrochemically mediated carbon dioxide separation with quinone chemistry in salt-concentrated aqueous media. *Nat. Commun.* **2020**, *11*, 1–11. [CrossRef]
17. Wu, F.; Zhao, G.; Wei, X. Electrocatalytic activity of multi-walled carbon nanotubes modified electrode for p-Benzenediol. *Chin. J. Anal. Chem.* **2004**, *08*, 1057–1060. [CrossRef]
18. Iijima, S. Helical microtubules of graphitic carbon. *Nature* **1991**, *354*, 56–58. [CrossRef]
19. Li, J.; Guan, Y.; Fu, K.; Su, Y.; Bao, L.; Wu, F. Applications of Carbon Nanotubes and Graphene in the Energy Storage Batteries. *Prog. Chem.* **2014**, *26*, 1233–1243. [CrossRef]
20. Voskian, S.; Hatton, T.A. Faradaic electro-swing reactive adsorption for CO_2 capture. *Energy Environ. Sci.* **2019**, *12*, 3530–3547. [CrossRef]
21. Yamamoto, T.; Etori, H. Poly (anthraquinone) s having a. pi.-conjugation system along the main chain. Synthesis by organometallic polycondensation, redox behavior, and optical properties. *Macromolecules* **1995**, *28*, 3371–3379. [CrossRef]
22. Liu, R.; Luo, Z.; Wei, Q. Preparation and Electrochemical Performance of PDAAQ/MWCNTs Composite. *J. Instrum. Anal.* **2016**, *35*, 765–768. [CrossRef]
23. Chen, Y.; Du, L.; Yang, P.; Sun, P.; Yu, X.; Mai, W. Significantly enhanced robustness and electrochemical performance of flexible carbon nanotube-based supercapacitors by electrodepositing polypyrrole. *J. Power Sources* **2015**, *287*, 68–74. [CrossRef]
24. Nagaoka, T.; Nishii, N.; Fujii, K.; Ogura, K. Mechanisms of reductive addition of CO_2 to quinones in acetonitrile. *J. Electroanal. Chem.* **1992**, *322*, 383–389. [CrossRef]
25. Guin, P.S.; Das, S.; Mandal, P.C. Electrochemical reduction of quinones in different media: A review. *Int. J. Electrochem.* **2011**, *2011*, 1–22. [CrossRef]
26. Apaydin, D.H.; Głowacki, E.D.; Portenkirchner, E.; Sariciftci, N.S. Direct electrochemical capture and release of carbon dioxide using an industrial organic pigment: Quinacridone. *Angew. Chem. Int. Ed.* **2014**, *53*, 6819–6822. [CrossRef] [PubMed]